Geotechnics for Developing Africa, Wardle, Blight & Fourie (eds) © 1999 Balkema, Rotterdam, ISBN 90 5809-082 5

Analysis of progressive failure of earth slopes by finite elements

J. B. Lechman
Geomechanics Research Center, Colorado School of Mines, Fort Collins, Golden, Colo., USA
D. V. Griffiths
Division of Engineering, Colorado School of Mines, Fort Collins, Golden, Colo., USA

ABSTRACT: Slope stability analysis is traditionally performed using limit equilibrium methods that have remained essentially unchanged for decades. While giving generally conservative estimates of safety factors, the traditional methods give no indication of progressive failure or how the yield spreads. This paper will describe some finite element analyses of slope stability using a relatively simple elasto-plastic, Mohr-Coulomb soil model. Within the finite element model however, gravity can be applied in different ways. For example, a "gravity turn on" procedure can be used where an initially weightless slope is instantaneoulsy subjected to self-weight loads. Alternatively, the slope can be "built-up" using an embanking procedure that creates the mesh one lift at a time, or similarly, by an excavation procedure. The different loading strategies and their influence on yeilding of the slope is highlighted in the paper through the use of contour plots of the failure criterion, which indicate the spread of yield within the slope and hence the location and shape of the potential failure surface. The influence of the loading strategies and dilation on the ultimate slope factor of safety is also examined.

1. INTRODUCTION

Prior to the advent of modern computing techniques, methods for determining the stability of slopes were, by necessity, a matter of making various assumptions to allow for the solving of equations of static equilibrium. The results of these limited, simplified analyses are presented in the form of charts of stability numbers (e.g. Taylor 1937, Bishop and Morgenstern 1960, Spencer 1967, Janbu 1967, Cousins 1978) from which the factor of safety can be determined based on the soil's strength properties and slope geometry. Common to all methods from which the charts are derived is the assumption that the slope can be divided into slices. After this initial step, further assumptions are made in order to solve the problem of static indeterminacy created by the side forces acting on the failing mass slice. While the variety of assumptions in dealing with these side forces are in generally good agreement with regards to overall safety factor, they may produce large discrepencies in the distribution of stresses throughout the failure mass (Whitman and Bailey 1967, Wright, et al. 1973). Cousins (1978) also lists several restictions to the use of these charts which deal with matters ranging from pore pressure, to limited slope angle range, to limited slope geometry, to limited or the lack of information about the failure surfaces. These charts are expedient and relatively easy to use, giving conservative values for the safety factor; however the aforementioned problems with limit equilibrium methods coupled with advances in computational ability beg the question of the possibility of more robust methods for analyzing slope stability.

One such method is the finite element method. The advantages of the method over limit equilibrium methods are stated by Griffiths (1996) as:

1. No assumption needs to be made in advance about the shape or location of the failure surface. Failure occurs "naturally" through the zones within the soil mass in which the soil shear strength is unable to sustain the applied shear stresses.

2. Since there is no concept of "slices" in the finite element approach there is no need for assumptions about slice side forces.

3. If realistic soil compressibility data is available, the finite element solutions will give

information about deformations at working stress levels.

4. The finite element method is able to monitor progressive failure up to and including overall shear failure.

This method has shown itself to be in good agreement with the various charts and proves to be very robust in that complications arising from the geometry of the slope and material property variations can be easily managed by it (Zienkiewicz et al. 1975, Griffiths 1980, 1989, Matsui and San 1992, Griffiths and Lane 1997). Advances made in refining the method and its applications may well prove to be a defining step in the maturation of soil mechanics. This paper examines the fourth item listed above via contour plots of the failure criterion as it is affected by gravity loading and dilation angle.

2. METHOD OF ANALYSIS

2.1 *Finite element method used*

The program is based closely on Program 6.1 in the text by Smith and Griffiths (1988)–the main difference being the ability to model more realistic geometries and better graphical output facilities. The programs are for 2-d (plane strain) analysis of elastic-perfectly plastic soils with a Mohr-Coulomb failure criterion. The programs use 8-node quadrilateral elements with reduced integration (4 Gauss-points per element) in both the stiffness and stress redistribution phases of the algorithm. A gravity 'turn-on' procedure generates nodal forces which act in the vertical direction at all nodes. These loads are applied in a single increment, or in percentage increments which generate normal and shear stresses at all the Gauss-points within the mesh. These stresses are then compared with the Mohr-Coulomb failure criterion. If the stresses at a particular Gauss-point lie within the Mohr-Coulomb failure envelope then that location is assumed to remain elastic. If the stresses lie on or outside the failure envelope, then that location is assumed to be yielding. Global shear failure occurs when a sufficient number of Gauss-points have yielded to allow a mechanism to develop.

The analysis is based on an iterative Modified Newton-Raphson method called the Viscoplastic algorithm (Zienkiewicz *et al* 1975). The algorithm forms the global stiffness matrix once only with all nonlinearity being transferred to the right hand side. If a particular zone within the soil mass is yielding, the algorithm attempts to redistribute those excess stresses by sharing them with neighboring regions that still have reserves of strength. The redistribution process is achieved by the algorithm generating self-equilibrating nodal forces which act on each element that contains stresses that are violating the failure criterion. These forces, being self-equilibrating, do not alter the overall gravity loading on the finite element mesh, but do influence the stresses in the regions where they are applied. In reducing excess stresses in one part of the mesh however, other parts of the mesh that were initially 'safe' may now start to violate the failure criterion themselves necessitating another iteration of the redistribution process. The algorithm will continue to iterate until both equilibrium and the failure criterion at all points within the soil mass are satisfied within quite strict tolerances. Convergence is achieved in a global sense by observing the change in nodal displacements from one iteration to the next. Convergence is satisfied when this change is less than 0.1%.

If the algorithm is unable to satisfy these criteria at all yielding points within the soil mass, 'failure' is said to have occurred. Failure of the slope and numerical non-convergence occur together, and are usually accompanied by a dramatic increase in the nodal displacements. Within the data, the user is asked to provide an iteration ceiling beyond which the algorithm will stop trying to redistribute the stresses. Failure to converge implies that a mechanism has developed and the algorithm is unable to simultaneously satisfy both the failure criterion (Mohr-Coulomb) and global equilibrium.

2.2 *Soil model*

An elastic-perfectly plastic (Mohr-Coulomb) model has been used in this work consisting of a linear (elastic) section followed by a horizontal (plastic) failure section.

The soil model used in this study consists of six parameters as shown in Table 1.

The dilation angle ψ affects the volume change of the soil during yielding. In this simple model ψ is assumed to be constant which is unrealistic, but will serve to show the affect of dilation on the final failure region.

The parameters c' and ϕ' refer to the cohesion and friction angle of the soil. Although a number of failure criteria have been suggested for use in representing the strength of soil as an engineering material, the one most widely used in geotechnical practice is due to Mohr-Coulomb. In terms of principal stresses and assuming a compression-negative sign convention, the criterion can be written as follows:

$$F = \frac{\sigma_1' + \sigma_3'}{2} \sin\phi' - \frac{\sigma_1' - \sigma_3'}{2} - c' \cos\phi' \qquad (1)$$

where c' and ϕ' represent the shear strength parameters of the soil and σ_1' and σ_3' the major

and minor principal effective stresses at the point under consideration. The failure function F can be interpreted as follows:

$F < 0$	inside M-C envelope (elastic)
$F = 0$	on M-C envelope (yielding)
$F > 0$	outside M-C envelope (yielding) and stresses must be redistributed

The unit weight γ assigned to the soil is important because it is proportional to the nodal loads generated by the gravity turn-on procedure.

In summary, the most important parameters in a finite element slope stability analysis are the unit weight γ which is directly related to the nodal forces trying to cause failure of the slope, and the shear strength parameters c' and ϕ' which measure the ability of the soil to resist failure.

2.3 *Determination of the factor of safety*

The Factor of Safety (FOS) of a soil slope is defined here as the factor by which the original shear strength parameters must be reduced to bring the slope to the point of failure. The factored shear strength parameters c'_f and ϕ'_f, are therefore given by:

$$c'_f = c'/FOS \tag{2}$$

$$\phi'_f = \arctan(\frac{\tan\phi'}{FOS}) \tag{3}$$

This method has been referred to as the 'shear strength reduction technique' (e.g. Matsui and San 1992) and allows for the interesting option of applying different factors of safety to the c' and $\tan\phi'$ terms. In this paper however, the same factor is always applied to both terms. To find the 'true' factor of safety, it is necessary to initiate a systematic search for the value of FOS that will just cause the slope to fail. This is achieved by the program solving the problem repeatedly using a sequence of user-specified FOS values.

However, when gravity is applied incrementally, the strength parameters are held constant and trail safety factor are held constant as loading is increased (compare Figures 1 and 4 or 2 and 3).

2.4 *Visualization technique*

For each successive trial safety factor or gravity load increment, the program described above gives a value of the failure criterion at each Gauss-point at convergence or failure (F). The coordinates of each Gauss-point and the corresponding value of F are then written to an output file which can be used in a commercial software package to produce contour plots which show the yielding regions of the slope. Of interest in the plots is the affects of an associated flow rule ($\phi = \psi$) on the spread of yield through the slope. It is also interesting to compare the results with traditional methods, namely those reported by Cousins (1978) which were arrived at by a modified Taylor method. The charts produced by Cousins are of particular interest because they not only give the stability factor but also the depth that the failure surface extends into the foundation of the slope. The finite element results can be compared to these results on the basis of overall factor of safety, or, when the failure criterion is contoured, the two methods can be compared on the basis of the location of the failure surface.

3. RESULTS

For the purposes of this paper, a simple, dry slope composed of a soil exhibiting friction and cohesion was analyzed. In general, this simplification is not necessary in the finite element method. However, when comparing the results to traditional methods, simplification is necessary on the grounds that limit equilibrium methods typically require this in order that the problems may be solved with ease. The choice of geometries corresponds with specific points on Cousins' charts at which the depth factor (D, the amount by which the height of the slope should be multiplied by to give the maximum height of the failure surface) can be determined explicitly. It should be noted that the definition of D in the context of Cousins' paper differs from other definitions of D. Cousins' paper uses D as a multiplier of the height of the slope (H) to give the maximum depth through which the failure surface passes and not as a multiplier of the height to give the depth to a solid base. Defined this way, a depth factor equal to 1 (D=1) implies a toe failure, where D=1.5 implies a failure surface that extends into the foundational material a distance equal to half the height and does not necessarily pass through the toe of the slope.

Furthermore, gravity loading methods are examined as they relate to the spread of yield and the shape and location of the yielding zone at failure.

Also, an examination of the influence of dilation on the spread of yield and the final state of the yielding zone at failure is contained here. The analyses in this paper have, by virtue of the variability of the amount of actual volume change, been limited to two simple cases. The cases considered are where $\psi = 0$ and $\psi = \phi'$. When the angle of dilation equals the internal angle of friction ($\psi = \phi'$) the flow rule is "associated"; thus direct comparisons to classical plasticity can be made. Some results of the analysis are as follows.

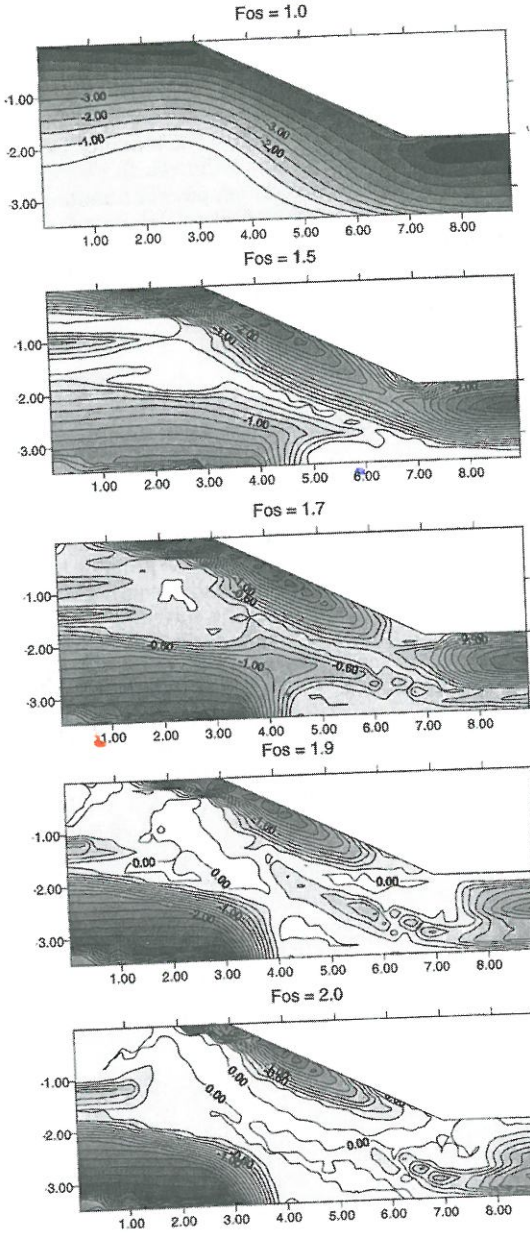

Figure 1. Embankment with a 2:1 slope, $c'/(\gamma H) = 0.15$, $\phi' = \psi = 16.7°$, and gravity applied instantaneously. Plots show contours of F at various FOS values. White regions are yielding $(F = 0)$.

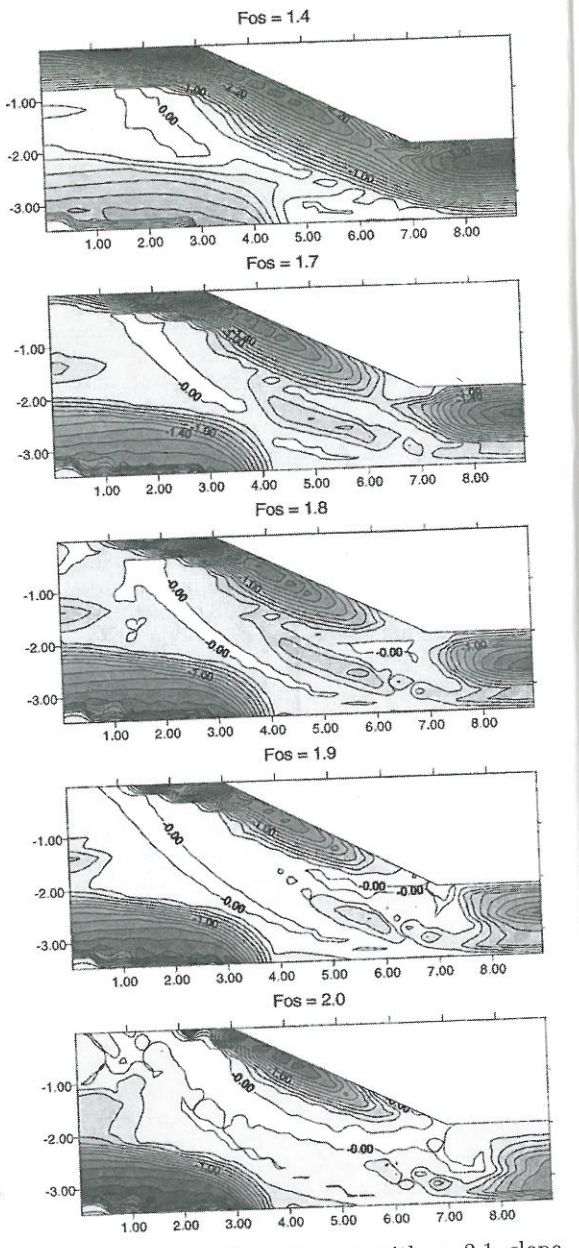

Figure 2. Embankment with a 2:1 slope, $c'/(\gamma H) = 0.15$, $\phi' = 16.7°$, $\psi = 0°$, gravity applied instantaneously. Plots show contours of F at various FOS values. White regions are yielding $(F = 0)$.

Figures 3 and 4 show zones of yielding for an embankment in which the soil properties remain constant and gravity is appled gradually.

4. CONCLUSIONS

Conclusions drawn from the investigation can be summarized as follows:

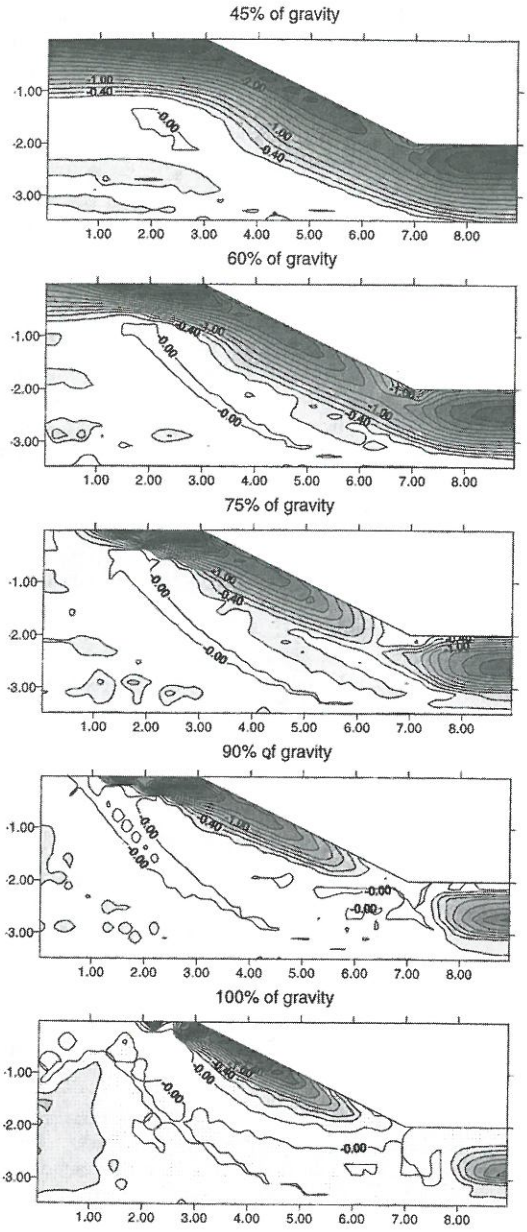

Figure 3. Embankment from Figure 2. Plots show contours of F at $FOS = 2$ with gravity applied incrementally. White regions are yielding ($F = 0$).

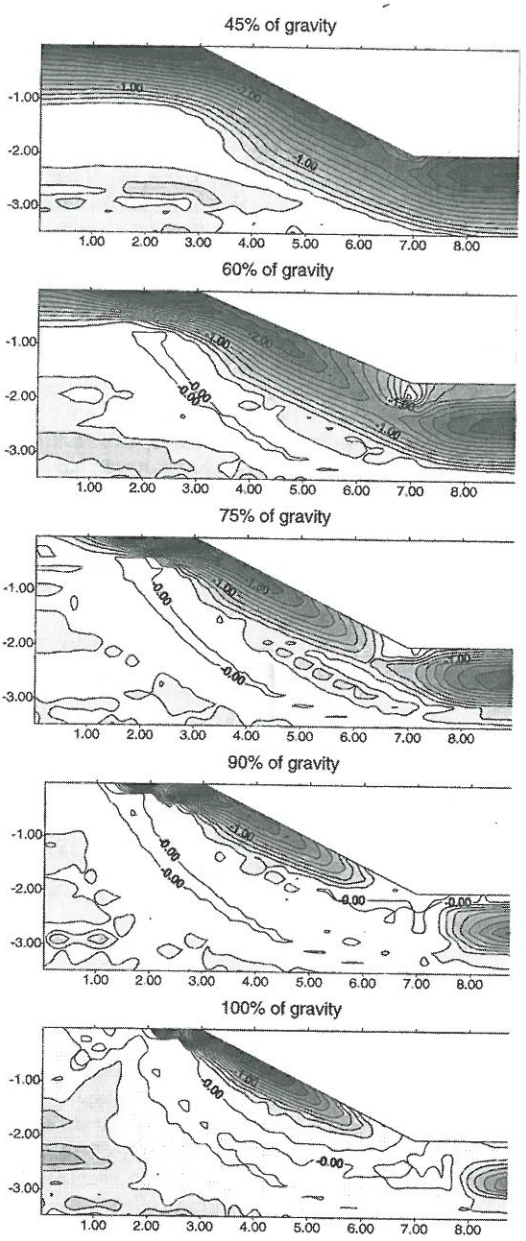

Figure 4. Embankment from Figure 1. Plots show contours of F at $FOS = 2$ with gravity applied incrementally. White regions are yielding ($F = 0$).

4.1 *Comparisons to Cousin's results*

1. Agreement was good for overall factor of safety. For the slope in the previous figures, Cousins' charts give a factor of safety of 2.03 compared to a factor of safety of 2.0 for the finite element analysis.

2. Cousins' charts also give a depth factor (D) of 1.25 which is approximately equal to that indicated by the finite element analysis. In general the finite element analysis showed more "transitional" regions between the explicit depth factors of $D = 1.0$, $D = 1.25$, $D = 1.5$ considered by Cousins. That is to say the bottom of the failure surface was not necessarily at a depth exactly equal to that implied by Cousins' depth factors. This is to be expected. As stated earlier, a priori knowledge of the failure surface is not required in finite element analysis as it is in limit equilibrium analysis; therefore the failure surface is allowed to develop "naturally." Although the two failure surfaces are not arrived at by the same means, the results indicate that Cousins' charts agree well with finite element results.

4.2 *Effects of Dilation*

1. Overall factor of safety did not vary significantly (less than 5%), for the same slope geometry and soil strength parameters, between the two cases.

2. At failure, the yielding zones of the two cases appear to be equivalent in size and shape (See Figures 1 and 2, $FOS = 2.0$).

3. Although the failure zones were similar at failure, the spread of yield could vary significantly between the two cases. It may be argued that the associated flow rule gives a more "satisfying" failure in that the spread of yield seems to occur in a more intuitive sense.

4. Under normal gravity conditions for a given slope geometry and soil strength parameters (represented by a factor of safety equal to one in this analysis), regions within the slope may already be experiencing stress conditions that promote yielding of the slope material. These regions were exceptionally large in slopes with relatively small safety factors (less than 1.75). Usually, these regions of yield appeared in the $\psi = 0$ case, and corresponded with a deep failure surface. For the associated flow rule case, this tendency was not as prominent indicating that the stress redistribution algorithm was more "effective" here.

4.3 *Effects of applying gravity incrementally*

Reults of this analysis are shown in figures 3 and 4. Here the trial safety factor was set to the value that caused failure in the analysis where gravity was applied all at once. The shear strength parameters were factored accordingly, and held constant. Gravity was then applied incrementally untill failure occurred at 100%.

1. Overall factor of safety was virtuall unchanged. For both dilation cases.

2. The general shape and location of the yielding zones appear to be equivalent at failure while some differences can be seen at other trial factor of safety values.

3. For both cases considered, a "deep" failure mechanism developed first, but apparently was resisted by frictional forces along the rigid foundation below. In general, when cohesion "dominates" the soils ability to resist shearing, a deep failure is expected. This is particularly evident in Taylor's chart for undrained clays ($\phi' = 0$), but is also apparent in Cousins' charts for frictional/cohesive materials.

REFERENCES

[1] A.W. Bishop and N.R. Morgenstern. Stability coefficients for earth slopes. *Géotechnique*, 10:129–150, 1960.

[2] B.F. Cousins. Stability charts for simple earth slopes. *J Geotech Eng, ASCE*, 104(2):267–279, 1978.

[3] D.V. Griffiths. *Finite element analyses of walls, footings and slopes.* PhD thesis, Department of Engineering, University of Manchester, 1980.

[4] D.V. Griffiths. Advantages of consistent over lumped methods for analysis of beams on elastic foundations. *Comm Appl Numer Methods*, 5(1):53–60, 1989.

[5] D.V. Grifiths. Fe-emb2 and fe-emb1: Slope stability software by finite elements. Technical Report GRC-96-37, Colorado School of Mines, 1996. Geomechanics Research Center.

[6] D.V. Grifiths and P.A Lane. Slope stability analysis by finite elements. Technical Report GRC-97-47, Colorado School of Mines, 1997. Geomechanics Research Center.

[7] N. Janbu. Slope stability computations. In *Soil Mech. and Found. Engrg. Rep.* Technical University of Norway, Trondheim, Norway, 1968.

[8] T. Matsui and K-C. San. Finite element slope stability analysis by shear strength reduction technique. *Soils Found*, 32(1):59–70, 1992.

[9] I.M. Smith and D.V. Griffiths. *Programming the Finite Element Method.* John Wiley and Sons, Chichester, New York, 2nd edition, 1988.

[10] E. Spencer. A method of analysis of the stability of embankments assuming parallel interslice forces. *Géotechnique*, 17(1):11–26, 1967.

[11] D.W. Taylor. Stability of earth slopes. *J. Boston Soc. Civ. Eng.*, 24:197–246, 1937.

[12] R.V. Whitman and W.A. Bailey. Use of computers for slope stability analysis. *J Soil Mech Found Div, ASCE*, 93(SM4):475–498, 1967.

[13] S.G. Wright, F.H. Kulhawy, and J.M. Duncan. Accoracy of equilibrium slope stability analysis. *J Soil Mech Found Div, ASCE*, 99(SM10):783–791, 1973.

[14] O.C. Zienkiewicz, C. Humpheson, and R.W. Lewis. Associated and non-associated viscoplasticity and plasticity in soil mechanics. *Géotechnique*, 25:671–689, 1975.